

1
2
3
4
5
6
7
8
9
10
11
12
13
14
15

Supporting Information

Single Pd Atoms Supported on Ultra-thin Bismuth Tungstate Nanosheets with Oxygen Vacancy as an Efficient Photocatalyst

Lizhen Hu^{1,2}, Xiaoxiang Huang¹, Qianqian Nie^{1,2}, Teng Wang¹, Penglei Liu¹, Jiayou
Liu¹, Zhongchao Tan^{2,3*}, Hesheng Yu^{1,2*}

1. School of Chemical Engineering and Technology, China University of Mining and Technology,
Xuzhou, Jiangsu, China, 221116

2. Department of Mechanical & Mechatronics Engineering, University of Waterloo, 200
University Avenue West, Waterloo, Ontario, Canada, N2L 3G1

3. Department of Energy and Power Engineering, Tsinghua University, Beijing, China, 100084

*Corresponding Authors: Dr. Z. Tan, Department of Mechanical & Mechatronics Engineering,
University of Waterloo, Waterloo, Ontario, Canada, N2L 3G1. Email: tanz@uwaterloo.ca;

Dr. H. Yu, School of Chemical Engineering and Technology, China University of Mining and
Technology, Xuzhou, Jiangsu, China, 221116. Email: heshengyu@cumt.edu.cn.

16 **1. Experimental section**

17 1.1 Materials and chemicals

18 Bismuth(III) nitrate pentahydrate ($\text{Bi}(\text{NO}_3)_3 \cdot 5\text{H}_2\text{O}$, $\geq 99\%$), sodium tungstate dihydrate
19 ($\text{Na}_2\text{WO}_4 \cdot 2\text{H}_2\text{O}$, $\geq 99\%$), and ethanol ($\geq 99.7\%$) were purchased from Sinopharm Chemical
20 Reagent Co., Ltd. (China); K_2PdCl_4 ($\geq 98\%$) was purchased from Shanghai Aladdin Biochemical
21 Technology Co., Ltd. All chemicals used in this work are of analytical grade and used as
22 received without further treatment. Ultrapure water with a resistivity of $18.2 \text{ M}\Omega \cdot \text{cm}^{-1}$ was
23 produced using a Direct-Q 5 UV System (Merck Millipore, Germany). All gases were purchased
24 from Xuzhou Special Gas Factory. The purities of O_2 and N_2 were 99.999%, and the NO
25 cylinder contained 1001 ppm NO balanced in N_2 .

26 1.2 Synthesis of photocatalysts

27 Synthesis of V_O -UBWO catalysts: The V_O -UBWO catalysts are synthesized through simple
28 self-assembly, following the steps shown in Fig. 1a. Briefly, 0.2 g of sodium oleate is dispersed
29 in 80 ml of ultrapure water at $50 \text{ }^\circ\text{C}$ by using continuous stirring magnetically for 10 min. After
30 that, the mixed solution is cooled to room temperature. Then 0.4 g of bismuth nitrate and 0.136 g
31 of sodium tungstate are added into the solution, followed by stirring magnetically for 30 min.
32 This precursor solution is transferred to a 100-ml Teflon-lined stainless steel autoclave. The
33 reactor is heated in an oven at $140 \text{ }^\circ\text{C}$ for 24 h, followed by natural cooling to room temperature.
34 The obtained mixed solution is centrifuged three times with ultra-pure water at $60 \text{ }^\circ\text{C}$, followed
35 by centrifugation three more times with an organic mixture, in which the volume ratio of

36 cyclohexane and ethanol is 1:4. Finally, the resultant precipitation is dried in the room air to
37 obtain V₀-UBWO samples.

38 Synthesis of Pd-V₀-UBWO catalysts: 0.6 g of the V₀-UBWO sample and 0.0032 g of
39 K₂PdCl₄ are dispersed in a beaker containing 180 ml of ultra-pure water and ultrasonicated for
40 10 min. The mixed solution is placed in an oil bath set to 70 °C and stirred magnetically for 8 h.
41 Then, the solution is centrifuged and washed using ultrapure water and absolute ethanol
42 alternatively for three times, followed by drying in a vacuum oven at 60 °C for 8 h. Finally, the
43 obtained powder is calcined in a tube furnace at 125 °C for 1 h with a heating rate of 5 °C/min in
44 a N₂ atmosphere to obtain Pd-V₀-UBWO SACs.

45 Synthesis of PdNPs-V₀-UBWO catalysts: 1 g of the V₀-UBWO sample is dispersed with
46 100 mL of ultra-pure water, which is stirred magnetically for 30 min to prepare Solution A.
47 0.005g of K₂PdCl₄ is dispersed with 10 ml of ultrapure water and ultrasonated for 3 min to
48 prepare Solution B. 0.0029 g of NaBH is then dispersed into 10 ml of ultrapure water followed
49 by ultrasonation for 3 min to form Solution C. After that, Solutions B and C are added in
50 sequence at an interval of 10 min to Solution A and stirred magnetically. Then the mixed
51 solution is aged for 2 h. Finally, the resultant solution is centrifuged using ultrapure water and
52 absolute ethanol, three times each, followed by drying in an oven at 70°C for 8 h to obtain
53 PdNPs-V₀-UBWO catalysts.

54 1.3 Characterizations

55 The crystal structures of the samples are characterized using X-ray diffraction (XRD,
56 Bruker D8-Advance, Germany) with Cu K α radiation (λ =1.5418 Å) over the 2 θ range of 5°-80°.
57 The morphologies and microstructures of the samples are examined using field emission

58 scanning electron microscopy (FE-SEM, Hitachi-SU8220, USA) and transmission electron
59 microscopy (TEM, Tecnai G2-F20 FEI, USA). The thickness of the UBWO nanosheets is
60 determined using AFM (Bruker Dimension Icon, GER). The Brunauer-Emmett-Teller (BET)
61 specific surface areas of the samples are measured by nitrogen adsorption-desorption
62 (Micromeritics ASAP 2460, USA). The elemental composition of the sample and the valence
63 state of Pd are determined using XPS (Thermo ECALAB 250xi system with a monochromatic Al
64 $K\alpha$ source, USA). Optical properties are determined using UV-vis diffuse reflectance spectra
65 (UV-vis DRS, Hitachi U-3900H, Japan). AC-HAADF-STEM images and EDS-mapping images
66 of the samples are taken using Titan Cubed Themis G2300 (JEM-ARM200F, Japan). The amount
67 of Pd element in the samples is determined using inductively coupled plasma mass spectrometry
68 (ICP-MS, Agilent 720ES(OES), USA). The concentrations of NO_3^- and NO_2^- in the used samples
69 are measured using IC (Thermo Scientific Aquion, USA). Radical species are detected using
70 ESR (Bruker EMXplus-6/1, Germany). The 5,5-dimethyl-1-pyrroline N-oxide (DMPO) is used
71 as a trapping agent for $\text{O}_2^{\cdot-}$ and OH^{\cdot} .

72 1.4 Photoelectrochemical measurements

73 Photocurrent, electrochemical impedance spectra (EIS), and Mott-Schottky tests are
74 conducted using an electrochemical workstation (CHI660E, Shanghai Chenhua, China) with a
75 standard three-electrode system. A saturated calomel electrode (SCE) and a Pt electrode are used
76 as the reference and counter electrodes, respectively. The electrolyte solution is 0.5M Na_2SO_4 .
77 The prepared catalysts are working electrode with an active area of *ca.* $1.0 \times 1.0 \text{ cm}^2$. The working
78 electrode is prepared following this procedure: First, 5 mg of the prepared photocatalyst and 20
79 μL of Nafion solution (DuPont, 5 wt.%) are dispersed into 1 ml of absolute ethanol by ultrasound

80 for 2 min. Then 200 μL of the prepared solution is coated onto an indium-tin oxide glass (ITO
81 $1\times 4\text{ cm}^2$) with an effective coating area of $1\times 1\text{ cm}^2$. Subsequently, the ITO glass is dried in an
82 oven at $90\text{ }^\circ\text{C}$ for 3 h to create the working electrode. A 300W xenon lamp with a 380 nm filter
83 is employed as the visible light source. The photocurrent is measured for 200 s at a bias voltage
84 of 0.5 V, and the lamp is turned on/off every 20 s. The EIS is performed at a bias voltage of 0.5 V
85 over the frequency range from 0.01 Hz to 10000 Hz. The Mott Schottky test is performed at a
86 frequency of 1000 Hz with voltages in the range of -0.6 -1.2 V.

87 1.5 Evaluation of Photocatalytic Activity for NO oxidation and RhB degradation

88 The photocatalytic oxidation of NO is carried out in a $5\times 10\times 0.5\text{ cm}$ rectangular ISO reactor.
89 A 300W xenon lamp (DP200A PN/2123XSL, Beijing, China) with a 380 nm cut-off filter is
90 placed vertically above the reactor as the light source. In a typical photocatalytic test, 0.08 g of
91 the prepared catalysts is coated onto a glass slide with an area of 50 cm^2 ($5\times 10\text{ cm}$, loading
92 capacity is $1.6\text{ mg}\cdot\text{cm}^{-2}$). More details can be found in an earlier publication¹.

93 In a typical photocatalytic test, the total flow rate of the mixed gas is controlled at 200
94 $\text{ml}\cdot\text{min}^{-1}$ by mass flow controllers (CS200A, Zhengzhou Ketan, China). The concentration of O_2
95 is 5% in the simulated gas. The relative humidity (RH) of the inlet gas is maintained at $60\pm 10\%$
96 and monitored using a hygrometer (UNI-T UT333, China). RH of 0% is achieved by removing
97 the moisture from the gas using silicone desiccants. RH of 100% is achieved by bubbling the gas
98 into water upstream the reaction system. The reaction system reaches adsorption-desorption
99 equilibrium after passing the gas mixture for 30 min, as indicated by the stable outlet NO
100 concentration of 48 ppm, which is monitored every 15 s using an FTIR analyzer (MKS MultiGas
101 2060, USA, with an accuracy of 2%). Then the xenon lamp is turned on for photocatalysis. The

102 concentrations of NO₂ and HNO₂ at the outlet of the reactor are also detected simultaneously
 103 every 15s using the FTIR analyzer.

104 Furthermore, the photocatalytic stability of the catalyst is evaluated by cyclic tests. After
 105 each cycle, the used catalysts are regenerated by UV light irradiation for 1 h to decompose
 106 deposited nitrate. There are three cycles in total.

107 When light is irradiated for a duration of t s, the total moles of input NO ($n_{NO,in}$), unremoved
 108 NO ($n_{NO,un}$), removed NO ($n_{NO,rem}$), generated NO₂ ($n_{NO_2,gen}$) and generated HNO₂
 109 ($n_{HNO_2,gen}$), conversion rate of NO (η_{NO}), removal efficiency of NO (β), the selectivity for the
 110 formation of NO₂ (S_{NO_2}), the selectivity for the formation of HNO₂ (S_{HNO_2}) in the reaction system
 111 are calculated as follows:

$$n_{NO,in} = \frac{P \times Q}{RT} \times \int_0^t C_{NO,in} dt \quad (S1)$$

$$n_{NO,un} = \frac{P \times Q}{RT} \times \int_0^t C_{NO,out} dt \quad (S2)$$

$$n_{NO,rem} = \frac{P \times Q}{RT} \times \left(\int_0^t C_{NO,in} \cdot dt - \int_0^t C_{NO,out} \cdot dt \right) \quad (S3)$$

$$n_{NO_2,gen} = \frac{P \times Q}{RT} \times \int_0^t C_{NO_2} dt \quad (S4)$$

$$n_{HNO_2,gen} = \frac{P \times Q}{RT} \times \int_0^t C_{HNO_2} dt \quad (S5)$$

$$\eta_{NO} = \frac{n_{NO,rem}}{n_{NO,in}} \times 100\% \quad (S6)$$

$$\beta = \frac{C_{NO,in} - C_{NO,out}}{C_{NO,in}} \times 100\% \quad (S7)$$

$$S_{NO_2} = \frac{n_{NO_2,gen}}{n_{NO,rem}} \times 100\% \quad (S8)$$

$$S_{HNO_2} = \frac{n_{HNO_2,gen}}{n_{NO,rem}} \times 100\% \quad (S9)$$

112 where P is the pressure in Pa; T is the temperature in the reaction system, the unit is K; R is the

113 molar gas constant with a value of $8.314 \text{ J}\cdot\text{mol}^{-1}\cdot\text{K}^{-1}$; and Q is the total flow rate of the gas. Its
 114 value is as follows: $Q = 200 \text{ ml}\cdot\text{min}^{-1} = 200 \times 10^{-6} / 60 \text{ m}^3\cdot\text{s}^{-1} = 3.333 \times 10^{-6} \text{ m}^3\cdot\text{s}^{-1}$; $C_{NO,in}$ is the
 115 concentration of input NO, $C_{NO,out}$ is the concentration of NO at the outlet, C_{NO_2} is the
 116 concentration of NO_2 at the outlet, C_{HNO_2} is the concentration of HNO_2 at the outlet in the
 117 reaction system, the unit is ppm, t is the light irradiates time, the unit is s.
 118 The moles of generated NO_3^- ($n_{NO_3^-,gen}$) and the selectivity for the formation of HNO_3 (S_{HNO_3})
 119 are calculated as follows:

$$n_{NO_3^-,gen} = \frac{c(NO_3^-)V}{M_{NO_3^-}} \quad (\text{S10})$$

$$S_{HNO_3} = \frac{n_{NO_3^-,gen}}{n_{NO,rem}} \times 100\% \quad (\text{S11})$$

120 Where $c(NO_3^-)$ is the concentration of NO_3^- measured by ion chromatograph, V is the volume of
 121 NO_3^- solution in the experiment, $M_{NO_3^-}$ is the relative atomic mass of NO_3^- .

122 The prepared catalysts are also tested under visible light irradiation for the degradation of
 123 RhB to expand its engineering potential. The light source is another xenon lamp (Yuming YM-
 124 GHX-V, Shanghai) with a 380 nm UV-filter. The light intensity is about 29.6 mW cm^2 as
 125 measured using a radiometer (Model FZ-A from Beijing Normal University, China). In a typical
 126 test, 25 mg of catalyst is dispersed into 50 ml of solution with a RhB concentration of $10 \text{ mg}\cdot\text{L}^{-1}$.
 127 Subsequently, the suspension is kept in the dark for 30 min to reach adsorption-desorption
 128 equilibrium. Then, the xenon lamp is turned on. 2-3 mL of the suspension is sampled every 10
 129 min. The supernatant is obtained by removing the particles from the sample by centrifugation.
 130 Finally, the concentration of RhB in the supernatant is measured using a UV-visible

131 spectrophotometer (Hitachi U-3900H, Japan). The RhB degradation efficiency is then calculated
132 using equation S12:

$$\eta_{RhB} = \frac{C_0 - C_t}{C_0} \times 100\% \quad (S12)$$

133 where η_{RhB} is the degradation efficiency of RhB in %, C_0 is the concentration of initial RhB in
134 mg/L, and C_t is the concentration of RhB after visible-light irradiation of t min.

135 Active species trapping experiment: Potassium dichromate ($K_2Cr_2O_7$) is used as scavengers
136 for e^- in the photocatalytic. The sample preparation follows a procedure that is similar to that for
137 the photocatalytic NO test, except for the addition of 1.6 mmol of $K_2Cr_2O_7$. In addition, the
138 photocatalytic activities of the Pd- V_O -UBWO catalysts for NO removal are tested in the absence
139 of O_2 and moisture to investigate the effects of $O_2^{\cdot-}$ and OH^{\cdot} on the photocatalytic activity.

140 1.6 Computational Methods

141 The DFT calculations are performed using the Vienna ab initio Simulation Package (VASP)
142 software². The exchange correlation function adopts the generalized gradient approximation
143 (GGA) of Perdew-Bruke-Emzerhof (PBE). The energy cut-off is set to 600 eV, and the
144 Monkhorst-Pack k-point is set to $3 \times 3 \times 1$. Self-consistent field (SCF) convergence criterion is 1.0
145 $\times 10^{-5}$ eV, and the break condition for the ionic relaxation loop is $0.05 \text{ eV} \cdot \text{\AA}^{-1}$. Considering the
146 Coulomb repulsion term (GGA+U) between electrons, the W and Pd atoms are assigned U_W of
147 6.2 eV and U_{Pd} of 3.6 eV, respectively³. The computational model of the BWO nanolayer uses
148 two BWO (001) planes to match the thickness of the prepared V_O -UBWO, and the vacuum layer
149 thickness is set to 20 Å. The formation energy is calculated using equation S2:

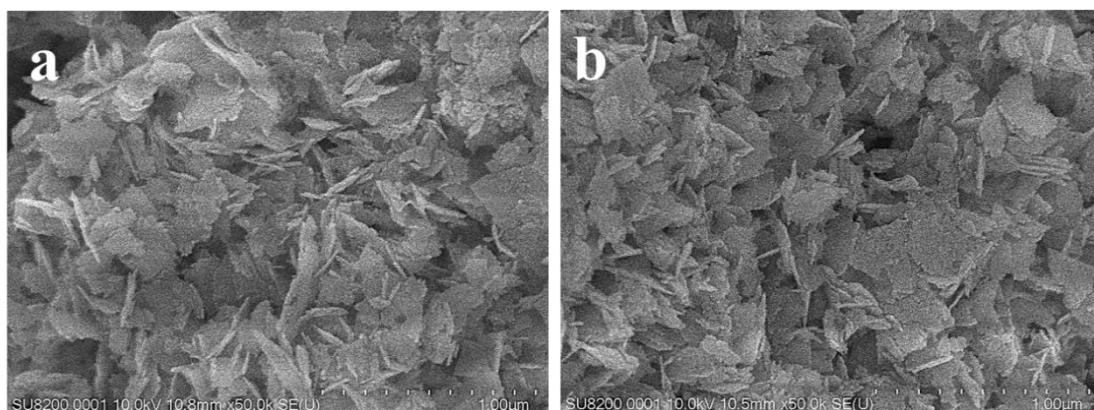
$$E_{for} = E_{Pd-V_O-UBWO} - (E_{Pd} + E_{V_O-UBWO}) \quad (S13)$$

150 where E_{Pd-V_O-UBWO} , E_{Pd} and E_{V_O-UBWO} are the total energies of Pd-V_O-UBWO, Pd atoms and

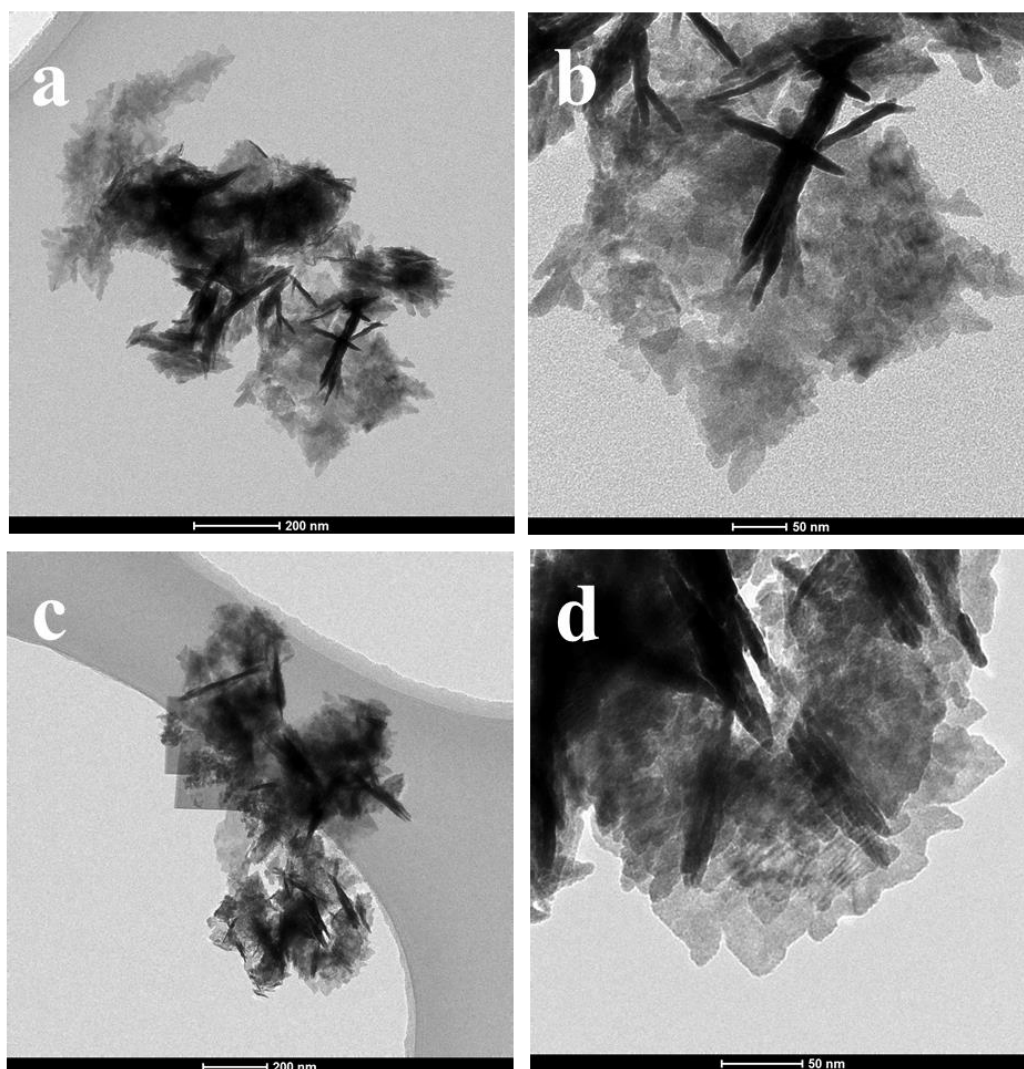
151 V_O-UBWO, respectively.

152

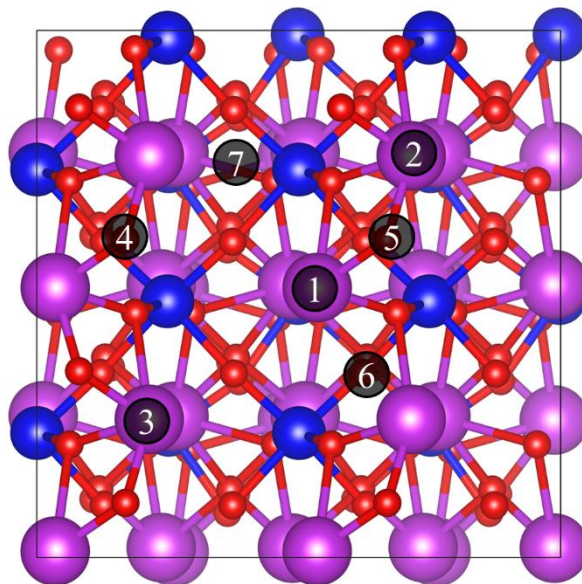
153 **Supplementary Figures**



155 **Figure S1. SEM images of (a) Vo-UBWO and (b) PdNPs-Vo-UBWO catalysts.**



158 **Figure S2. TEM images of (a, b) Vo-UBWO and (c, d) PdNPs-Vo-UBWO catalysts.**



159

160 Figure S3. The 7 Possible positions of single Pd atoms on V_{O} -UBWO (O vacancy at position 6).

161 Selected Pd loading positions: positions 1, 2, 3 are at the top of Bi atom at different distances

162 from the O vacancy; positions 4, 5 are at the top of O atom at different distances from the O

163 vacancy, positions 6 is the O vacancy on the surface of UBWO; positions 7 is the bridge between

164 the unbonded Bi atom and O atom bit (above the midpoint of the yellow dotted line in the

165 Figure).

166

167 Table S1. The formation energies of single Pd atoms adsorbed at different positions on
 168 the V_O-UBWO surface.

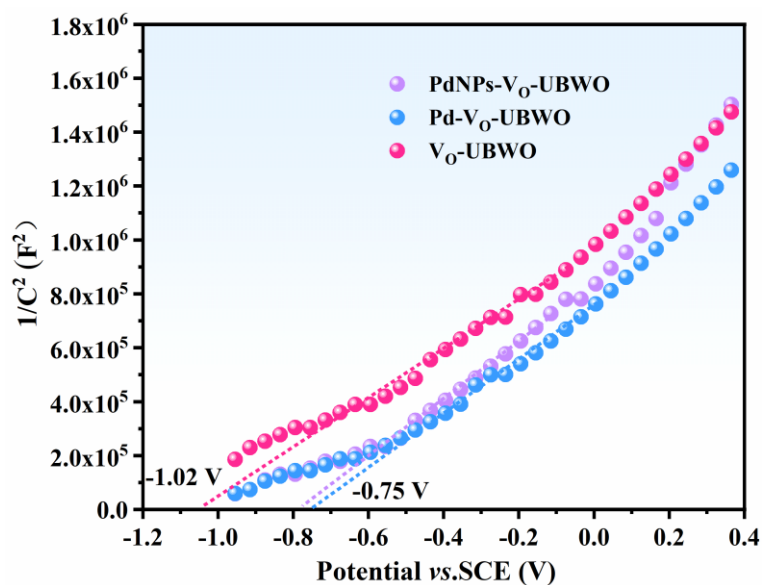
positions	formation energies (eV)
1	-1.167
2	-1.865
3	-2.105
4	-1.477
5	-1.542
6 (O vacancy)	-2.495
7	-1.931

169

170 Table S2. Pd amount of different chemical valences in Pd-BWO and PdNPs-BWO catalysts

Samples	Pd-V _O -UBWO (%)	PdNPs-V _O -UBWO (%)
Pd species		
Pd ²⁺	5.7	0
Pd ⁺	76.8	32.4
Pd ⁰	17.5	67.6

171



172

173 Figure S4. The Mott Schottky curves of V₀-UBWO, Pd-V₀-UBWO, and PdNPs-V₀-UBWO

174

catalysts.

175

$$E_{NHE} = E_{SCE} + 0.24 V^4 \quad (S14)$$

for n-type semiconductors,

$$E_{CB} = E_{fb} - 0.30 V^{5,6} \quad (S15)$$

$$E_{CB} = E_g + E_{VB} \quad (S16)$$

176 where E_{NHE} is normal hydrogen electrode potential (NHE);

177 E_{SCE} is SCE potential;

178 E_{CB} is conduction band potential;

179 E_{fb} is flat band potential; E_g is the band gap;

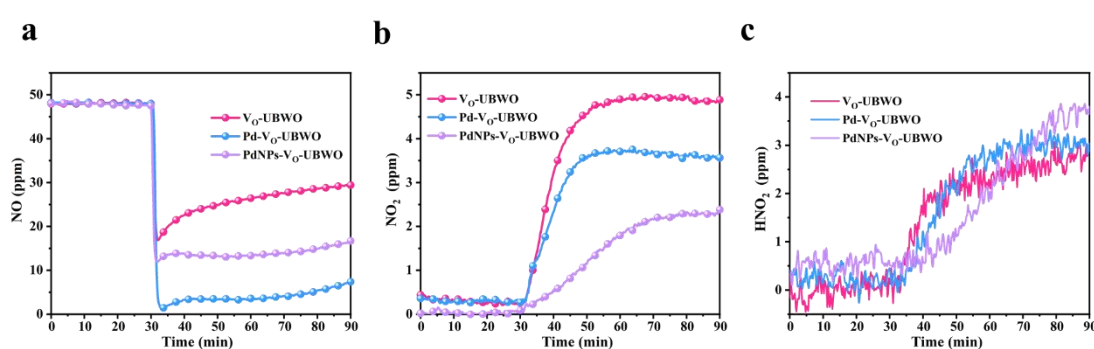
180 E_{VB} is valence band potential.

181

182 Table S3. Band structures of V₀-UBWO, Pd-V₀-UBWO, and PdNPs-V₀-UBWO catalysts

Sample	V ₀ -UBWO	Pd-V ₀ -UBWO	PdNPs-V ₀ -UBWO
E _g (eV)	2.87	2.63	2.80
CB (V)	-1.08	-0.81	-0.83
VB (V)	1.79	1.82	1.97

183



184

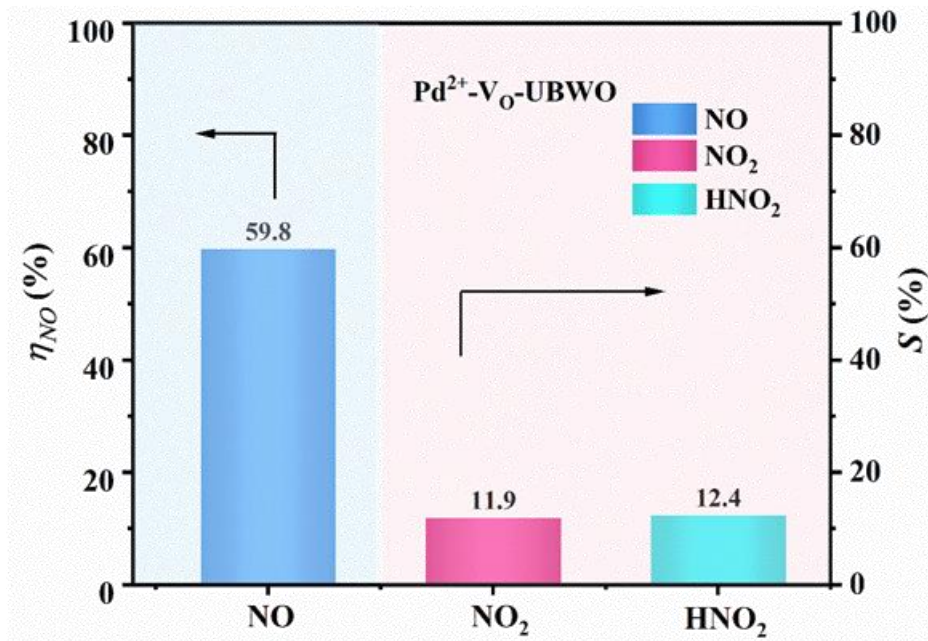
185 Figure S5. (a) NO removal, (b) NO₂ generation, (c) HNO₂ generation of photocatalytic NO of the

186 V₀-UBWO, Pd-V₀-UBWO and PdNPs-V₀-UBWO catalysts under visible light irradiation for 1h

187 at a $C_{NO,in}$ of about 48 ppm.

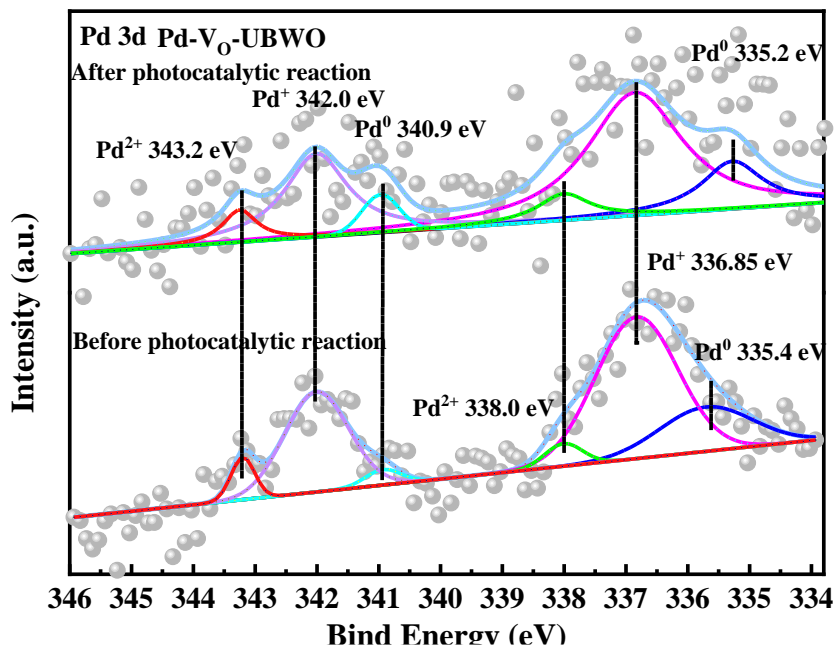
188 Pd²⁺-V₀-UBWO catalyst was synthesized following a procedure reported earlier in the
 189 literature.⁷ First, 0.6 g of V₀-UBWO catalyst was dispersed in 180 ml ultrapure water by
 190 ultrasonication for 5 min and kept magnetically stirred for 30 min, and 0.0032 g of K₂PdCl₄ was
 191 dispersed in 10 ml of ultrapure water by ultrasonication. Then, the solution was added dropwise to
 192 the V₀-UBWO solution, followed by magnetic stirring for 30 min. Then the obtained mixed
 193 solution was aged for 2 h. After that, the solution was centrifuged three times with ultrapure water
 194 and anhydrous ethanol, respectively. Finally, the obtained solid was dried in an oven at 60 °C for 8
 195 h.

196



197

198 Figure. S6 The η_{NO} , S_{NO_2} and S_{HNO_2} for photocatalytic NO removal of Pd²⁺-V_o-UBWO catalyst.

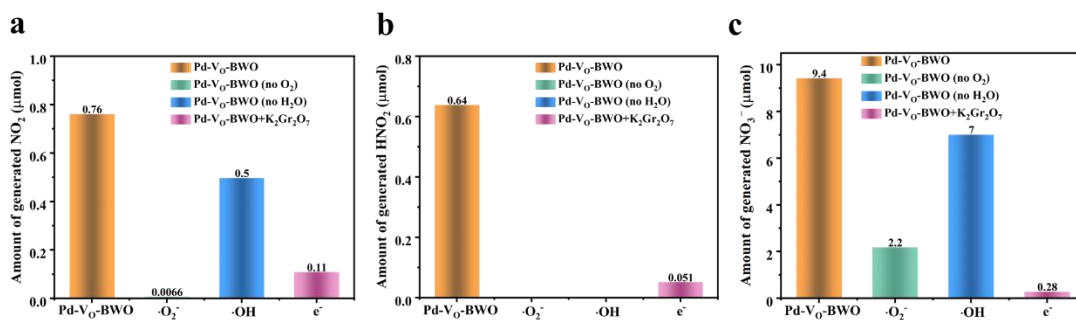


199

200 Figure.S7 Pd 3d XPS spectra of Pd-V_o-UBWO catalysts before and after irradiation under

201 visible light for 1h with inlet NO concentration of 48 ppm.

202



203

204

Figure S8. (a) The NO₂ generation, (b) HNO₂ generation and (c) NO₃⁻ generation in Pd-V₀-

205

UBWO catalyst under the conditions of adding K₂Gr₂O₇ and removing O₂, moisture.

206

References

207

1. Y. Cui, T. Wang, J. Liu, L. Hu, Q. Nie, Z. Tan and H. Yu, *Chem. Eng. J.*, 2021, **420**.

208

2. S. Kirkpatrick, C. D. Gelatt and M. P. Vecchi, *Science*, 1986, **9**, 339-348.

209

3. W. Setyawan, R. M. Gaume, S. Lam, R. S. Feigelson and S. Curtarolo, *ACS Comb Sci*, 2011, **13**, 382-390.

210

4. Y. Cui, X. Huang, T. Wang, L. Jia, Q. Nie, Z. Tan and H. Yu, *Carbon*, 2022, **191**, 502-514.

211

5. N. Tian, H. Huang, C. Liu, F. Dong, T. Zhang, X. Du, S. Yu and Y. Zhang, *J Mater Chem A*, 2015, **3**, 17120-17129.

212

213

6. K. Li, Y. He, P. Chen, H. Wang, J. Sheng, W. Cui, G. Leng, Y. Chu, Z. Wang and F. Dong, *J Hazard Mater*, 2020, **392**, 122357.

214

215

7. Z. Ni, F. Dong, H. Huang and Y. Zhang, *Catal. Sci. Technol.*, 2016, **6**, 6448-6458.

216

217

